

Stability conditions for the traveling pulse: Modifying the restitution hypothesis

Eric Cytrynbaum^{a)}

Institute of Theoretical Dynamics, University of California, Davis, California 95616

James P. Keener

Department of Mathematics, University of Utah, Salt Lake City, Utah 84112

(Received 6 November 2001; accepted 9 July 2002; published 23 August 2002)

As a simple model of reentry, we use a general FitzHugh–Nagumo model on a ring (in the singular limit) to build an understanding of the scope of the restitution hypothesis. It has already been shown that for a traveling pulse solution with a phase wave back, the restitution hypothesis gives the correct stability condition. We generalize this analysis to include the possibility of a pulse with a triggered wave back. Calculating the linear stability condition for such a system, we find that the restitution hypothesis, which depends only on action potential duration restitution, can be extended to a more general condition that includes dependence on conduction velocity restitution as well as two other parameters. This extension amounts to unfolding the original bifurcation described in the phase wave back case which was originally understood to be a degenerate bifurcation. In addition, we demonstrate that dependence of stability on the slope of the restitution curve can be significantly modified by the sensitivity to other parameters (including conduction velocity restitution). We provide an example in which the traveling pulse is stable despite a steep restitution curve. © 2002 American Institute of Physics. [DOI: 10.1063/1.1503941]

The question of spiral and scroll wave breakup has recently received increased attention in the discussion of the onset of fibrillation. A theoretical understanding of the transition from ventricular tachycardia to ventricular fibrillation is currently being constructed in terms of the loss of stability of a steadily rotating spiral or scroll wave. While numerical simulations of cardiac tissue models are capable of demonstrating spiral and scroll wave breakup, there is no consensus as to exactly what determines the loss of stability. Although several candidates have been proposed^{1–4} (see Ref. 5 for a recent review), in the work presented here, we focus on one in particular, the restitution hypothesis. In the last few years, this hypothesis has gained credibility through experimental advances,^{6–8} numerical simulations,^{9,10} and analytical results^{11,12} and is being promoted as the new touchstone for anti-arrhythmic drugs.^{5,13} Courtemanche *et al.*, in particular, demonstrated the validity of the hypothesis for a simple model of reentry. However, the stability result in that paper hints at the main problem with the hypothesis. First, the bifurcation through which stability is lost is degenerate (an infinite dimensional Hopf bifurcation), meaning that the hypothesis lacks robustness and might fail for slightly more complicated systems. Second, two physiological properties, action potential duration (APD) restitution and conduction velocity (CV) restitution, are the two main physiological parameters that play an important role in the stability calculation but one of them (CV restitution) drops out of the final stability condition. In the present study, we “unfold” the bifurcation, deriving a

more general stability condition which reintroduces the dependence on conduction velocity restitution and gives a modified restitution hypothesis. An example illustrates the extent to which the modified restitution hypothesis deviates from the original one.

I. INTRODUCTION

The principle assumption underlying the restitution hypothesis, first adopted by Nolasco and Dahlen,¹⁴ is that the duration of an action potential (APD) for a single cell is dependent on the preceding recovery period or diastolic interval (DI) only. The function relating APD to DI is called the APD restitution curve (sometimes simply the restitution curve) and, assuming the cell experiences a periodic stimulus, can be used to define a map from the previous APD to the next APD. The magnitude of the derivative of this map at the fixed point determines the stability of the fixed point; less than unity implies stability with instability otherwise. This derivative condition is referred to here as the *restitution condition*.

The restitution hypothesis proposes that the stability not only of isolated cells but also of reentrant signals is determined by the restitution condition. That is, if the slope of the restitution curve is greater than unity for a steady periodic signal then that signal is unstable. It is thought to be relevant in a wide range of contexts including a pulse propagating on a ring of tissue as well as spiral and scroll waves in higher dimensions.

It should be noted that the problem of defining the restitution curve for a given system is not a trivial problem. For the simplest case of an isolated cell undergoing periodic

^{a)}Electronic mail: eric@math.utah.edu

stimulus, one must decide when a cell is excited and when it is recovering. Choosing a cutoff transmembrane potential allows for a clear designation but the resulting restitution curve can be cutoff dependent.¹⁵ Moreover, the restitution curve may not be well defined in the sense that one value of DI might correspond to two different values of APD as has been observed previously.¹¹ Fortunately, in theoretical studies where the excitable system is composed of a fast and a slow subsystem (as in FitzHugh–Nagumo), this problem is (mostly) avoided. Cardiac cells appear to behave similarly.

For an isopotential isolated cell satisfying the principle assumption of APD dependence and subject to an external periodic stimulus, the restitution condition is the correct condition for stability of the steady response. Nolasco and Dahlen,¹⁴ Guevara *et al.*,¹⁵ and, more recently, Yehia *et al.*¹⁶ among others use this approach to understand the appearance of alternation in the APD of a cell under periodic stimulus.

However, when such cells are coupled together to form a ring or a sheet, the coupling can influence the internal dynamics so that restitution is no longer a property of individual cells. Thus, there are two types of systems that can be studied—those for which coupling has (almost) no influence on repolarization and those for which it does. The former are characterized by having a phase wave for a wave back while the latter are characterized by having a trigger wave for a wave back. The designation *phase wave*, in contrast with *trigger wave*, refers to the fact that repolarization occurs according to a cell's internal "excitation clock" rather than by being triggered by its repolarized neighbors.

With this in mind, it should be clear that for reentrant signals propagating through tissue, the validity of the restitution condition is a bit more subtle. Early in the last century, Mines observed reentry in a "one-dimensional" ring of cardiac tissue.¹⁷ Several studies have focused on this simple model of reentry to draw conclusions about the nature of the "alternans" instability,^{9,18} building an argument in favor of the restitution hypothesis which claims the restitution condition is the correct stability condition. One of the few analytical results on the problem of stability of reentry added much credibility to the hypothesis. Courtemanche *et al.* demonstrated that the restitution condition is the correct stability condition for a FitzHugh–Nagumo pulse on a ring in the singular limit with a phase wave for a wave back. Despite this apparent progress toward establishing the restitution hypothesis, the Courtemanche result hints at its underlying weakness. Its narrow context (singular wave front, phase wave back) and the nature of the bifurcation through which stability is lost (an infinite dimensional Hopf bifurcation) are signs of a degenerate phenomenon. Does the restitution hypothesis still hold for slightly different systems?—the non-singular case?—a triggered wave back instead of a phase wave?

In an attempt to better understand the restitution hypothesis, we examine the same system but with a triggered back instead of a phase wave back. (A technical discussion of the difference between a phase wave back and a triggered wave back is given in the Appendix.) The relevance of this change to cardiac tissue is that an argument can be made for the predominance of triggered wave backs in spiral waves, at

least in regions close to the core. The absence of the effects of spatial coupling in the model proposed by Courtemanche *et al.* has been addressed in other studies by modifying the integral-delay equation from Ref. 11 through the addition of an APD coupling term.¹⁹ Here, we return to the derivation of the integral-delay equation, this time allowing for the presence of a triggered back, and proceed to derive a map that generalizes the integral-delay equation. In this way, the effect of coupling is carried through from the original PDE and not added to the derived model after the fact.

Using this map, we derive a stability criterion for a FitzHugh–Nagumo pulse on a ring with a triggered wave back. As with the phase wave case, when the condition for the loss of stability and the restitution condition coincide, the bifurcation is degenerate in the same way (an infinite dimensional Hopf bifurcation). However, for a generic choice of parameter values, the loss of stability is through a one-dimensional Hopf bifurcation which is consistent with the numerical observation that APD coupling breaks the degeneracy of the bifurcation.¹⁹ Furthermore, the stability condition deviates from the restitution condition and a dependence on conduction velocity restitution is introduced. This new stability condition generalizes the restitution condition but complicates the question of how to "stabilize" an unstable reentrant rhythm. Readers not interested in the details of the stability calculation can refer to the derived stability and instability criteria at the end of Sec. II for a summary of the main results and skip to Sec. III for a relatively self-contained discussion of the results.

II. THE SINGULAR FITZHUGH–NAGUMO SYSTEM

A. Reduction from FitzHugh–Nagumo

We begin with the FitzHugh–Nagumo system on a ring of length L ,

$$\epsilon \frac{\partial v}{\partial \tau} = \epsilon^2 \frac{\partial^2 v}{\partial x^2} + f(v, w), \quad (1)$$

$$\frac{\partial w}{\partial \tau} = g(v, w), \quad (2)$$

$$v, \frac{\partial v}{\partial x}, w|_{x=0} = v, \frac{\partial v}{\partial x}, w|_{x=L},$$

where space has been scaled by the space constant of the medium so that L is measured in nondimensional units. We assume that f has three zeros, $v_-(w)$, $v_0(w)$, and $v_+(w)$, for each w in some bounded interval (w_{\min}, w_{\max}) and only one zero for w outside of that interval (the standard cubic-like function). g is chosen so that the system has a single spatially homogeneous stable solution at $(v, w) = (v_-(0), 0)$ (see Fig. 1 for the phase plane).

In order to formally reduce the problem to a discussion of the movement of fronts and backs, we take the limit $\epsilon \rightarrow 0$. This limit is singular and must be analyzed in two distinct scalings. The outer scaling is the one given above (setting $\epsilon = 0$ in Eq. (1)) and indicates that the transmembrane potential, v , resides on one of two stable solution branches, $v_+(w)$ or $v_-(w)$, of the equation $f(v, w) = 0$. We refer to

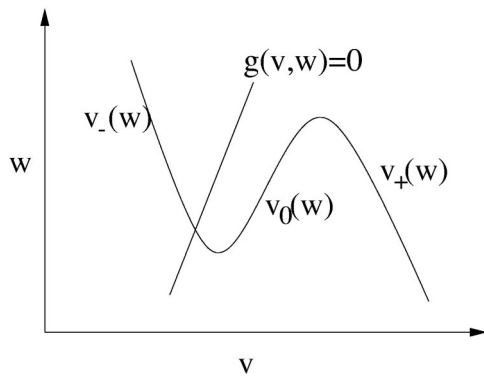


FIG. 1. The phase plane for a general FHN model. The nullcline of $f(v, w)$ is labeled by its three branches, $v_-(w)$, $v_0(w)$, and $v_+(w)$. $g(v, w)$ is usually taken to be linear.

$v_+(w)$ as the excited branch and to $v_-(w)$ as the recovery branch. Evolution of w on these branches is described by Eq. (2) where v is replaced by the appropriate branch value ($v_+(w)$ or $v_-(w)$).

The inner scaling is found by rescaling both time and space by a factor of ϵ . Taking the limit $\epsilon \rightarrow 0$ in this scaling gives a bistable equation (functions of the inner variables are denoted with capital letters):

$$\frac{\partial V}{\partial t} = \frac{\partial^2 V}{\partial z^2} + f(V, W), \tag{3}$$

where W is constant on the fast time scale given by t . The existence and stability of traveling waves to such an equation is well known for W in the bistable interval.²⁰ These traveling waves play the role of transition layers from the excited branch to the recovery branch. The W value at a transition layer determines the speed and direction of that layer, allowing for the definition of the speed function, $c(W)$. Note that this speed function is implicitly a function of f . An example of a speed function, $c(W)$, calculated explicitly, is given for $f(v, w) = v(1-v)(v-1/10) - w$ in Fig. 2.

The state of the singular FitzHugh–Nagumo system (SFHN) can be expressed in terms of $w(x, \tau)$ and the location of all transition layers which we denote by $\phi_i(\tau)$ with i

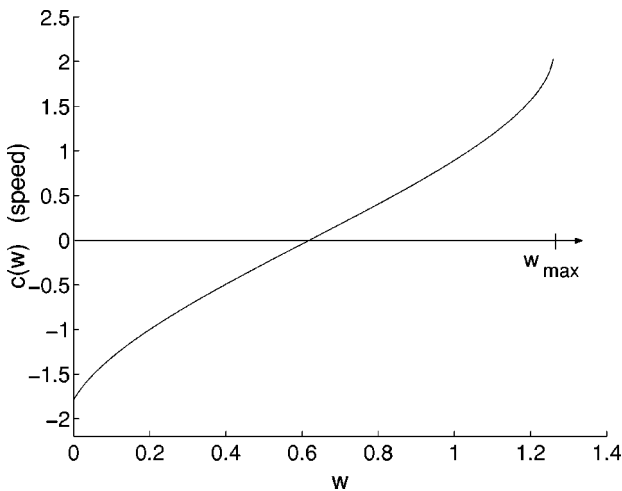


FIG. 2. The speed function for cubic $f(v, w)$.

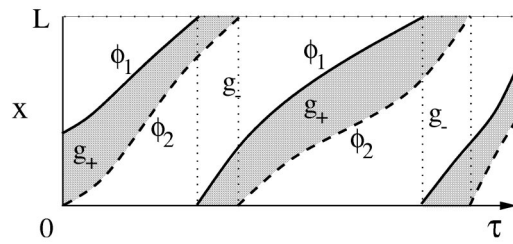


FIG. 3. Schematic plots of the positions of the front, $\phi_1(\tau)$ (solid line), and the back, $\phi_2(\tau)$ (dashed line). The appropriate w dynamics between the curves are specified by g_+ (shaded region) and g_- (unshaded region).

taking values between one and the number of layers (necessarily even). In addition, we must specify the state (excited or recovering) of the system on the intervals between layers. Thus, the singular FitzHugh–Nagumo dynamics are described by

$$\frac{\partial w}{\partial \tau}(x, \tau) = g(v_{\pm}(w), w), \tag{4}$$

$$\phi_i'(\tau) = (-1)^i c(w(\phi_i, \tau)), \tag{5}$$

where $x, \phi_i(\tau) \in [0, L]$ with the end points of that interval identified. The sign in Eq. (5) assumes that the origin is excited or, more precisely, that the transition layer at ϕ_1 is oriented such that the interval to its left is excited and the one to its right is recovering.

Equation (5) is only valid for $w(\phi(\tau), \tau) \in (w_{\min}, w_{\max})$. It is possible that at some time τ , $w(\phi(\tau), \tau) = w_{\max}$ so that the back becomes a phase wave (see the appendix for more on phase waves). As we are interested in linear stability of a pulse with a triggered back, we assume the phase wave scenario never arises.

B. The system as an iterated map

Being interested in stability of the traveling pulse, we begin with the SFHN system, (Eqs. (4) and (5)), with two transition layers, a front at ϕ_1 and a back at ϕ_2 , both traveling to the right:

$$\frac{\partial w}{\partial \tau}(x, \tau) = g(v_{\pm}(w), w),$$

$$\phi_1'(\tau) = -c(w(\phi_1, \tau)),$$

$$\phi_2'(\tau) = c(w(\phi_2, \tau)).$$

In the first equation, $v_+(w)$ is used on the interval $(\phi_1(\tau), \phi_2(\tau))$ and $v_-(w)$ is used on the complementary interval $(\phi_2(\tau), \phi_1(\tau))$ (see Fig. 3 for clarification).

$\phi_1(\tau)$ is the location of a front (w is relatively low) that goes from the upper to the lower branch with increasing x and $\phi_2(\tau)$ is the location of a back (w is relatively high) facing in the opposite direction.

Our goal is to replace this system of equations with an iterated map for which the traveling pulse is a fixed point and stability analysis amounts to calculating the eigenvalues of the linearization of the map at this fixed point. One approach is to calculate $\phi_1(\tau)$ and $\phi_2(\tau)$ from a given initial condition from $\tau=0$ until the time at which each returns to the

point at which it started. Continuing, one could calculate these functions through a second rotation and so on. A map can be defined from (ϕ_1, ϕ_2) on one rotation to (ϕ_1, ϕ_2) on the following rotation. In Fig. 3, this would mean defining a map that has the first continuous segments of ϕ_1 and ϕ_2 as input and the second continuous segments as output. The difficulty with this map is that the argument is a pair of functions whose domain cannot be specified in advance because the time required for the front and back to make one full rotation may vary from rotation to rotation. To avoid this difficulty, we invert these functions so that the interval $[0, L]$ is the domain of the input functions on every rotation.

To be more precise, the map we define takes the pair $(T(x), t(0))$ to the pair $(S(x), s(0))$ where $T(x)$ and $S(x)$ are the first and second arrival times of the front at the point x , respectively, and $t(0)$ and $s(0)$ are the first and second arrival times of the back at $x=0$. We assume that ϕ_1 is piecewise monotone increasing and invert it to get $T(x)$ on the interval $[0, L]$ (without loss of generality, $T(0)=0$). We can define $t(x)$ similarly (by inverting ϕ_2) but we only require a single point, $t(0)$, which is found by solving $\phi_2(\tau_0)=0$ and setting $t(0)=\tau_0$. The set of all such pairs, $(T(x), t(0))$ with $T(x)$ smooth, is the space on which the map is to be defined. Given an initial condition to the SFHN system, we can calculate the corresponding initial point, $(T(x), t(0))$. The evolution of the SFHN system can be translated into a map as describe in the remainder of this section.

In general, the speed function for propagating transition layers, $c(w)$, is a monotone function for $0 \leq w < w_{\max}$ with values in the range $[c_{\min}, c_{\max})$ where $c_{\min} := c(0)$ and $c_{\max} := c(w_{\max})$. Thus, instead of tracking w everywhere in space and evaluating c only at the layers, we can derive an equation for c everywhere in space and eliminate w from consideration. This amounts to keeping track of refractoriness in terms of potential propagation speed instead of using an explicit refractory variable. Taking derivatives with respect to τ we get

$$\frac{\partial c}{\partial \tau} = c'(w) \frac{\partial w}{\partial \tau} = c'(w) g_{\pm}(w).$$

Monotonicity of $c(w)$ guarantees that we can rewrite this as

$$\frac{\partial c}{\partial \tau} = G_{\pm}(c). \tag{6}$$

Note that $G_+(c) > 0$ for $c < c_{\max}$ corresponding to increasing refractoriness while in the excited state, while $G_-(c) < 0$ for $c > c_{\min}$ corresponding to recovery (see Fig. 4).

At a point x , for times between $\tau = T(x)$ and $\tau = t(x)$, the evolution of c is determined by $\partial c / \partial \tau = G_+(c)$. Provided only with $T(x)$ and $t(0)$, we are missing two vital pieces of information. First, we require an initial condition, $c(x, T(x))$, for Eq. (6). Second, we do not know the time at which the evolution of c switches from the “+” branch to the “-” branch (with the exception that at $x=0$, we know the switch occurs at $\tau = t(0)$).

The initial condition is calculated from $T(x)$ using the fact that

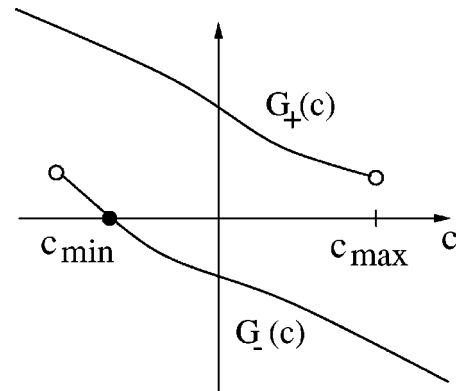


FIG. 4. A schematic diagram of the “+” and “-” branch dynamics in terms of c —essentially, the original formulation of the SFHN system turned on it’s side. On the “+” branch, c increases until it falls off at $c = c_{\max}$. On the “-” branch, c approaches the steady state at c_{\min} .

$$c(x, T(x)) = -1/T'(x).$$

Finding the time, $t(x)$, at which the evolution of c switches branches, is a more complicated matter. Notice the apparent paradox in that we need to know $t(x)$ in order to know when to stop using $G_+(c)$ in calculating c . But to calculate $t(x)$, we require $c(x, \tau)$ for an unknown stretch of time.

The solution to this problem is to temporarily ignore the fact that the evolution of c switches branches at $t(x)$. At each point x , we allow c to evolve according to G_+ until it falls off the end of the excited branch. Integrating $c(x, \tau)$ in time from $T(x)$ to the end of the branch, we get a curve $t_{\max}(x)$ that serves as an upper bound on $t(x)$ where $t_{\max}(x)$ is defined as the value of τ for which $c(x, \tau)$ hits the end of the branch. Once this upper bound is established, we can find $t(x)$ by solving

$$t'(x) = 1/c(x, t(x)). \tag{7}$$

Note that $c(x, \tau)$ as calculated previously is only valid up to $\tau = t(x)$ and must be redefined for values of $\tau > t(x)$ once $t(x)$ is properly determined (see Fig. 5).

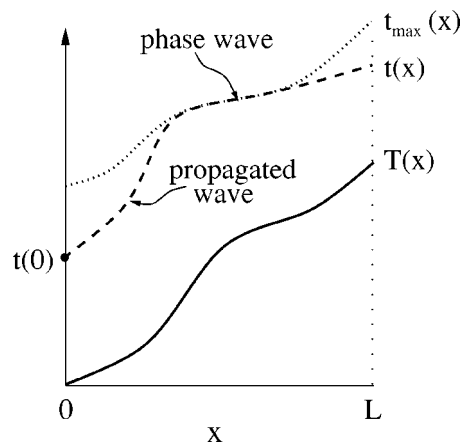


FIG. 5. An illustration of the steps involved in calculating the map. The slope of $T(x)$ gives an initial condition for $c(x, \tau)$ which is integrated until t_{\max} at which time it falls off the “+” branch. $t(0)$ is used as an initial condition for integrating $t(x)$ which is defined by the integration (triggered sections) or by t_{\max} (phase wave sections).

If $t(x_0) = t_{\max}$ for some x_0 , Eq. (7) is no longer valid and the wave back switches from a triggered wave to a phase wave. As we are interested in the case of triggered waves only, we assume $t(x) \neq t_{\max}$ for all x .

In a similar fashion, without the complication of phase waves, we can follow the same procedure starting with $t(x)$ and $S(0)$ (by periodicity, $S(0) = T(L)$) to find $S(x)$ and $s(0)$ which we define, respectively, as the second arrival time of the front at x and the second arrival time of the back at $x = 0$.

This multi-step calculation defines a map

$$F: \begin{pmatrix} T(x) \\ t(0) \end{pmatrix} \mapsto \begin{pmatrix} S(x) \\ s(0) \end{pmatrix}.$$

Notice that this map can be interpreted as a generalization of the APD restitution curve in that it maps the APD at one point ($t(0) - T(0)$) to the next APD at that point ($s(0) - S(0)$). Of course, information from the whole ring ($T(x)$) is required to define the map making it much more complicated to characterize (i.e., it is no longer a one-dimensional map).

The traveling pulse solution can be represented by a straight line $T(x) = x/c_0$ where c_0 is the traveling speed of the pulse. The calculation of c_0 and $t(0)$ is carried out in the Sec. II C.

C. The traveling pulse as a fixed point

Even if the traveling pulse has a triggered wave back, it is possible that, after a perturbation, the back might transiently convert to a phase wave. However, for small enough perturbations of the traveling pulse, this ought not happen. Thus, we need not worry about phase waves which allows the expression of the map to be simplified enormously. The equation for c on the excited branch, $\partial c / \partial \tau = G_+(c)$, can be used to derive a single equation for $t(x)$ without going through the intermediate step of solving for $c(x, \tau)$:

$$t(x) - T(x) = \int_{-1/T'(x)}^{1/t'(x)} \frac{1}{G_+(c)} dc. \tag{8}$$

Similarly, we can derive an equation for $S(x)$:

$$S(x) - t(x) = \int_{1/t'(x)}^{-1/S'(x)} \frac{1}{G_-(c)} dc. \tag{9}$$

Thus, given $T(x)$ and $t(0)$ we can use Eqs. (8) and (9) to find $t(x)$ and $S(x)$, respectively. Notice that these two equations are integro-differential equation of a peculiar type.

The traveling pulse can be expressed as $T(x) = x/c_0$ where the traveling speed c_0 is not yet known. The map $F: (T, t(0)) \rightarrow (S, s(0))$ must give $S(x) = T(x) + L/c_0$ so the pulse is a fixed point up to some spatially uniform shift (L/c_0). To completely determine the pulse we must calculate c_0 and $t(0)$.

Because $t(x) = t(0) + x/c_0$, Eq. (8) requires that

$$t(0) = \int_{-1/T'(0)}^{1/t'(0)} \frac{1}{G_+(c)} dc = \int_{-c_0}^{c_0} \frac{1}{G_+(c)} dc.$$

Similarly, from Eq. (9) we see that

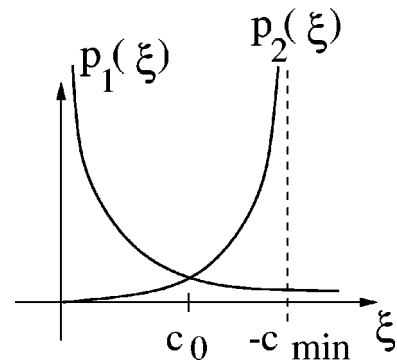


FIG. 6. Plots of $p_1(\xi)$ and $p_2(\xi)$ with a unique intersection at c_0 for the case $c_{\max} > -c_{\min}$.

$$S(0) = t(0) + \int_{c_0}^{-c_0} \frac{1}{G_-(c)} dc.$$

By periodicity, the front must be at $x=0$ and $x=L$ simultaneously so that $S(0) = T(L) = L/c_0$. These requirements on S implicitly define c_0 through

$$\int_{-c_0}^{c_0} \frac{1}{G_+(c)} dc + \int_{c_0}^{-c_0} \frac{1}{G_-(c)} dc = \frac{L}{c_0}.$$

To find conditions under which a solution to this equation exists, we define the following two functions

$$p_1(\xi) = \frac{L}{\xi}, \quad \xi > 0, \tag{10}$$

$$p_2(\xi) = \int_{-\xi}^{\xi} \frac{1}{G_+(s)} ds + \int_{\xi}^{-\xi} \frac{1}{G_-(s)} ds \tag{11}$$

for $0 < \xi < \max(-c_{\min}, c_{\max})$. Note that $p_1(\xi) \rightarrow \infty$ as $\xi \rightarrow 0^+$, $p_1(\xi) \rightarrow 0$ as $\xi \rightarrow \infty$ and the function $p_1(\xi)$ is monotone decreasing for all $\xi > 0$. Conversely, $p_2(0) = 0$ and $p_2(\xi)$ is increasing for $0 < \xi$. When integrating the second of the two integrals in Eq. (11), there are two possibilities.

The first possibility is that $c_{\max} > -c_{\min}$. In this case, p_2 is only defined up to $\xi = -c_{\min}$ and has a singularity at that point. In this case, p_1 and p_2 intersect so that a traveling pulse with a triggered wave back necessarily exists (see Fig. 6).

The second possibility is that $c_{\max} \leq -c_{\min}$ in which case p_2 is only defined up to c_{\max} . The existence of a traveling pulse with a triggered back requires $p_2(c_{\max}) > L/c_{\max}$. We can always choose L sufficiently small so that the wave back is a triggered wave. For large L , the wave back is a phase wave.

In either case, the value of ξ at the intersection of p_1 and p_2 is the desired c_0 .

Summarizing, the first passage of the traveling pulse takes the form

$$T^*(x) = \frac{x}{c_0},$$

$$t^*(x) = \frac{x}{c_0} + t_0,$$

while the second passage is given by

$$S^*(x) = \frac{x}{c_0} + \frac{L}{c_0},$$

$$s^*(x) = \frac{x}{c_0} + \frac{L}{c_0} + t_0,$$

where

$$t_0 = \int_{-c_0}^{c_0} \frac{dc}{G_+(c)}$$

and c_0 solves

$$\int_{-c_0}^{c_0} \frac{1}{G_+(c)} dc + \int_{c_0}^{-c_0} \frac{1}{G_-(c)} dc = \frac{L}{c_0}.$$

D. Stability of the traveling pulse

To determine the stability of the traveling pulse calculated in Sec. II C, we perturb $T^*(x)$ and t_0 by a small amount and determine the influence of the perturbation on $S(x), s(0)$,

$$T(x) = T^*(x) + \epsilon A(x),$$

$$t(x) = t^*(x) + \epsilon a(x) + O(\epsilon^2),$$

$$S(x) = S^*(x) + \epsilon B(x) + O(\epsilon^2),$$

$$s(x) = s^*(x) + \epsilon b(x) + O(\epsilon^2).$$

In fact, we are only required to specify $T(x)$ and $t(0)$ but in anticipation of the structure of $t(x)$ and $S(x)$, we name the resulting perturbations first and proceed to find expressions for them. We seek the linearization of F which takes $(A(x), a(0))$ to $(B(x), b(0))$.

Linearizing Eq. (8), we find that

$$a(x) = \int_0^x e^{k_1(s-x)} (k_1 A(s) - k_2 A'(s)) ds + a(0) e^{-k_1 x},$$

where

$$k_1 = \frac{G_+(c_0)}{c_0^2} > 0, \quad k_2 = \frac{G_+(c_0)}{G_+(-c_0)} > 0.$$

Note that the initial data for the map requires both $A(x)$ and $a(0)$.

Similarly,

$$B(x) = \int_0^x e^{k_3(s-x)} (k_3 a(s) - k_4 a'(s)) ds + A(L) e^{-k_3 x},$$

where

$$k_3 = -\frac{G_-(-c_0)}{c_0^2} > 0, \quad k_4 = \frac{G_-(-c_0)}{G_-(c_0)} > 0.$$

To determine the stability of the fixed point (traveling pulse), we look for eigenvalues and eigenfunctions of the map by setting $A(x) = e^{\alpha x}$ and $a(0) = a_0$ where α might be complex. For a perturbation of this form (assuming $\alpha \neq -k_1, -k_3$), we get

$$a(x) = \beta e^{\alpha x} + (a_0 - \beta) e^{-k_1 x}$$

where $\beta = (k_1 - \alpha k_2)/(k_1 + \alpha)$ and

$$B(x) = C(\alpha) e^{\alpha x} + C_1 e^{-k_1 x} + C_3 e^{-k_3 x},$$

where

$$C(\alpha) = \frac{k_3 - \alpha k_4}{k_3 + \alpha} \beta, \quad C_1 = \frac{k_3 + k_1 k_4}{k_3 - k_1} (a_0 - \beta)$$

and

$$C_3 = e^{\alpha L} - C(\alpha) - C_1.$$

In order for $(e^{\alpha x})$ to be an eigenvector, it must be that

$$\begin{pmatrix} B(x) \\ a(L) \end{pmatrix} = \lambda \begin{pmatrix} e^{\alpha x} \\ a_0 \end{pmatrix}.$$

The first component of this equation forces $C_1 = C_3 = 0$, which means $a_0 = \beta$ and $C(\alpha) = e^{\alpha L}$. Thus the eigenvalues are of the form $\lambda = e^{\alpha L}$ where α satisfies the characteristic equation $C(\alpha) = e^{\alpha L}$.

We rewrite the characteristic equation in terms of a new set of parameters:

$$\frac{1 - \alpha h_1 - \alpha h_3}{1 + \alpha h_2 + \alpha h_4} = e^{\alpha L}, \tag{12}$$

where

$$h_1 = \frac{c_0^2}{G_+(-c_0)}, \quad h_2 = \frac{c_0^2}{G_+(c_0)},$$

$$h_3 = -\frac{c_0^2}{G_-(c_0)}, \quad h_4 = -\frac{c_0^2}{G_-(-c_0)}.$$

Interpretation of these parameters, which play a central role in determining stability, is addressed more carefully in Sec. III.

Equation (12) determines α (infinitely many values) and therefore the eigenvalues, $\lambda = e^{\alpha L}$. Stability requires that $|\lambda| < 1$ for every eigenvalue λ , or equivalently $\text{Re}(\alpha) < 0$ for every solution, α , to Eq. (12).

Note that $\alpha = 0$ is always a solution to Eq. (12) and corresponds to the constant eigenfunction. This means that the traveling pulse is unique only up to phase shifts, a result of the fact that the SFHN system is autonomous.

A few facts about $C(\alpha)$ that will be useful in understanding stability should be stated at this point. Because $C(\alpha)$ is the product of linear fractional functions with no singularities in the right half plane (including the imaginary axis), the image of that region is a compact set. Moreover, because $1/h_1$ and $1/h_3$ are both positive, the origin is covered (twice) by that region. This structure allows us to restrict our analysis to the imaginary axis. In particular, if the image of the imaginary axis under $C(\alpha)$ lies completely within the unit circle (except for the origin which maps to one and is always a root), so does the entire right half plane. Because e^α maps the right half plane outside the unit circle, there can be no solution, α , to Eq. (12) with $\text{Re}(\alpha) > 0$ (see Fig. 7). Alternately, if the image of the imaginary axis lies completely outside the unit circle, there can be no roots of the characteristic equation in the left half plane.

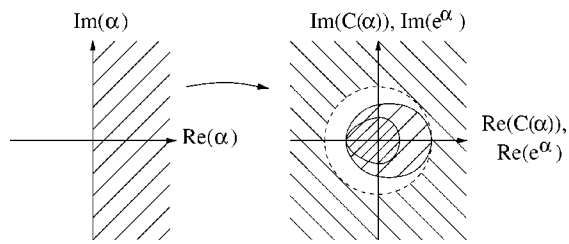


FIG. 7. A representation of the functions $C(\alpha)$ and e^α for values of h_i , $i = 1, 2, 3, 4$ satisfying the stability criterion. The image of the right half plane under $C(\alpha)$ is shaded by lines with positive slope; the solid curve is the image of the imaginary axis. Note the double cover of the origin. The image of the right half plane under e^α is shaded by lines with negative slope; the dashed curve is the image of the imaginary axis. Clearly, there can be no point in the right half plane (aside from the origin) that maps to the same point under both functions.

For the image of the imaginary axis to be contained inside the unit circle we require $|C(iv)|^2 < 1$, where

$$|C(iv)|^2 = \frac{1 + (h_1^2 + h_3^2)v^2 + h_1^2 h_3^2 v^4}{1 + (h_2^2 + h_4^2)v^2 + h_2^2 h_4^2 v^4}.$$

Clearly, the numerator and denominator agree at $v=0$ which, as previously mentioned, is always a root of the characteristic equation. The following two stability conditions describe the two possibilities for the rest of the imaginary axis (either inside or outside the unit circle).

Stability criterion. The image under $C(\alpha)$ of the imaginary axis (excluding the origin) lies entirely inside the unit circle ($|C(iv)|^2 < 1$) if the following two conditions are satisfied:

$$\begin{aligned} h_1^2 + h_3^2 &< h_2^2 + h_4^2, \\ h_1 h_3 &< h_2 h_4. \end{aligned} \quad (13)$$

When the parameters h_1 , h_2 , h_3 , and h_4 satisfy these conditions, stability of the traveling pulse is guaranteed.

Instability criterion. The image under $C(\alpha)$ of the imaginary axis (excluding the origin) lies entirely outside the unit circle ($|C(iv)|^2 > 1$) if the following two conditions are satisfied:

$$\begin{aligned} h_1^2 + h_3^2 &> h_2^2 + h_4^2, \\ h_1 h_3 &> h_2 h_4. \end{aligned} \quad (14)$$

When the parameters satisfy these conditions, any nonconstant perturbation of the traveling pulse is amplified (all but the trivial eigenvalue are greater than one).

To understand how stability might be lost, we examine how roots of the characteristic equation cross from the left to the right half of the complex plane. A crossing of any root must correspond to some value v for which $|C(iv)| = 1$. At this value of v ,

$$(h_1^2 + h_3^2 - h_2^2 - h_4^2)v^2 + (h_1^2 h_3^2 - h_2^2 h_4^2)v^4 = 0.$$

If this polynomial is not identically zero, there can be at most one pair of conjugate roots of this equation. Thus, stability can be lost only through one pair of roots changing the sign of their real part or all roots changing the sign of their real parts simultaneously. In the language of bifurcations, stabil-

ity can be lost either through a simple (one-dimensional) Hopf bifurcation or through an infinite dimensional Hopf bifurcation. The conditions for an infinite dimensional Hopf bifurcation are

$$\begin{aligned} h_1^2 + h_3^2 &= h_2^2 + h_4^2, \\ h_1 h_3 &= h_2 h_4. \end{aligned} \quad (15)$$

Recall that the bifurcation found by Courtemanche *et al.* was of the latter type.

III. DISCUSSION

A. Testing the restitution hypothesis

In the stability analysis of Courtemanche *et al.*,¹¹ a similar characteristic equation was derived and it was found that the slope of the restitution curve is the crucial determinant of stability. In particular, $dAPD/dDI < 1$ is a necessary and sufficient condition for stability of the traveling pulse. Although this dependence on the slope of the APD restitution curve might have been anticipated by the stability criterion for one-dimensional maps, it is surprising that this factor alone plays the same role in the more complicated context of the singular limit of the PDE flow. Furthermore, Courtemanche *et al.* find that when stability is lost, it is always through an infinite dimensional Hopf bifurcation which, they note, is probably not the case for the original PDE system. Motivated by these facts, we attempt to reinterpret our stability condition in terms of these restitution properties. We begin with a brief description of restitution and how it appears in the discussion of stability in general.

For an isolated cell stimulated at sufficiently low frequency, the duration of excitation (action potential duration or APD) is steady from one stimulus to the next. If the pacing frequency increases, the APD begins to alternate between long and short time intervals. In the standard analysis, the APD is assumed to be a function of the amount of time spent recovering prior to a stimulus (the diastolic interval or DI). This function is referred to as the restitution curve. Theory predicts that the APD undergoes a period doubling bifurcation when the restitution curve achieves a slope of one at the fixed point.

From the perspective of a single cell on a ring of coupled cells, a steady pulse looks like the periodic stimulus in the isolated cell experiment. In this case, the period of stimulation is determined by the speed of the pulse and the size of the ring. Although the coupling changes the dynamics, one is tempted to think only in terms of isolated cell dynamics. (In fact, this is not such a bad approximation when the back is a phase wave because the phase wave assumption amounts to assuming that repolarization is intrinsic to a cell and is not driven by coupling. This assumption brings the PDE system conceptually closer to the ordinary differential equation system and is essential to the results of Courtemanche *et al.*¹¹) For a given set of parameters, each cell is excited for a period of time (APD) and recovering for a period of time (DI). If the traveling pulse is steady, every cell has the same APD and the same DI. Changing a parameter of the system gives a different APD and DI. Each of these two quantities is ex-

explicitly a function of the underlying parameters and thus it is possible to derive an implicit relation between APD and DI. We refer to this relation as the restitution curve despite the subtle difference between it and its more dynamical relative of the same name which describes the dynamic response of an isolated cell to stimulus.

It is important to point out at that this notion of restitution curve does not provide a dynamic description in the sense that it does not predict how a pulse converges to a steady APD–DI pair; it merely describes the steady state relationship. In fact, the map, F , defined in Sec. II B gives the dynamic relationship between successive turns of the pulse. Despite this limitation, one can still test to see if the condition $dAPD/dDI > 1$ corresponds to the loss of stability of a traveling pulse. In the rest of this section, we calculate the slope of the restitution curve for the reduced model, expressing it in terms of $h_1, h_2, h_3,$ and h_4 and demonstrate that the correspondence between the slope of the restitution curve and the loss of stability for the traveling pulse is not generic.

Before calculating the restitution curve, a brief description of the parameters, h_i , will be useful. Recall the definitions of h_i :

$$h_1 = \frac{c_0^2}{G_+(-c_0)}, \quad h_2 = \frac{c_0^2}{G_+(c_0)},$$

$$h_3 = -\frac{c_0^2}{G_-(c_0)}, \quad h_4 = -\frac{c_0^2}{G_-(-c_0)}.$$

Referring to Eqs. (8) and (9), APD can be expressed as

$$APD = \int_{-c_0}^{c_0} \frac{1}{G_+(c)} dc \tag{16}$$

and DI can be expressed as

$$DI = \int_{c_0}^{-c_0} \frac{1}{G_-(c)} dc. \tag{17}$$

Interpreting these parameters, we see that h_1 and h_2 measure the sensitivity of APD to changes in parameters of the model measured in terms of their effect on propagation speed; h_3 and h_4 measure the sensitivity of DI to similar changes. h_1 and h_4 measure changes due to dynamics near the wave front, while h_2 and h_3 measure changes due to dynamics near the wave back.

To illustrate, suppose we start with a particular set of parameters and the corresponding traveling pulse solution. Making a slight change in some parameter of the model induces a slight change in the traveling pulse solution and, in particular, its speed of propagation. Now, suppose that h_2 is large. Our small parameter change generates a relatively large change in the contribution of the integrand in Eq. (16) at the upper limit of integration (the wave back). Thus, we might say that if h_2 is large then APD is sensitive to parameter changes that influence late pre-repolarization dynamics. In an ionic model, this might manifest itself as a high sensitivity in Ca^{2+} current to changes in some underlying parameter of the model. Another way to describe this is to say that a small increase in some parameter leads to a disproportion-

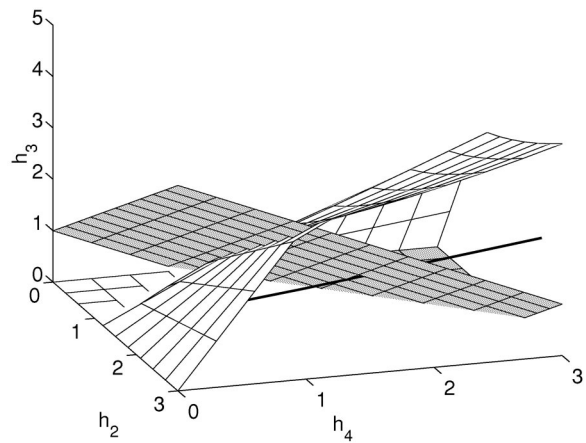


FIG. 8. Splitting up parameter space. The region below the dark gray surface is the region of guaranteed stability. The region above the light gray surface is that of guaranteed instability. Above the white surface is the region predicted by the restitution hypothesis to give stability and below it is predicted instability. The curve corresponds to h values for the piecewise linear FHN model—notice the segment in the “stable but predicted unstable” region.

ate increase in APD due to a slow region in the phase space that was not accessed before the parameter change. The other three parameters can be interpreted similarly.

We now return to the restitution curve calculation. Note that APD and DI are both functions of c_0 . This allows us to determine the derivative of APD with respect to DI implicitly through c_0 :

$$\frac{dAPD}{dc_0} = \frac{h_1 + h_2}{c_0^2}, \quad \frac{dDI}{dc_0} = \frac{h_3 + h_4}{c_0^2},$$

$$\frac{dAPD}{dDI} = \frac{h_1 + h_2}{h_3 + h_4}. \tag{18}$$

With this quantity in hand, we can explore parameter space to test the restitution hypothesis. Motivated by the infinite dimensional Hopf bifurcation found in Ref. 11, we begin with parameter values satisfying Eq. (15) (the case of an infinite dimensional Hopf bifurcation in our system). These bifurcation conditions are equivalent to

$$(h_1 - h_2)(h_1 + h_2) = (h_4 - h_3)(h_4 + h_3),$$

$$h_1 - h_2 = h_4 - h_3.$$

If the loss of stability corresponds to an infinite dimensional Hopf bifurcation with $h_1 \neq h_2$ then $dAPD/dDI = 1$. This seems to support the restitution hypothesis but has the same degeneracy difficulties that were found in the case with phase wave backs.

In fact, there are parameter values for which the traveling pulse is stable with $dAPD/dDI > 1$. To see that this is the case, Fig. 8 presents a plot of parameter space that shows the regions in question. By rescaling h_1, h_2, h_3, h_4 by h_1 , we reduce the dimension of the parameter space from four to three.

The two surfaces in Fig. 8 represent two sets of inequalities. The restitution condition is represented by the gray wire mesh with the region above the surface corresponding to a

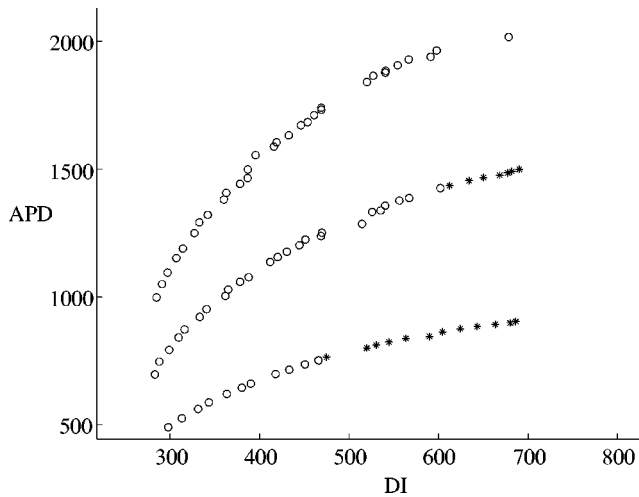


FIG. 9. APD restitution curves for piecewise linear FHN for three different values of μ (from bottom to top, $\mu=3,5,7$). Stars correspond to points at which the slope is less than one, open circles correspond to points at which the slope is greater than one. Despite the open circles (achieving slopes greater than eight), all traveling pulses were found to be stable.

restitution curve with a slope less than one. We refer to this region as the *predicted stability region*. The region below the gray surface is the *predicted instability region*. The region below the white surface satisfies the stability criterion and thus corresponds to parameter values which guarantee a stable traveling pulse. The surface corresponding to the instability condition is located above the white surface but is left out for clarity.

As an example, we offer a family of models which, for certain parameter choices, violates the stability predictions of the restitution condition. This family demonstrates the existence of a stable traveling pulse despite a restitution curve with a slope significantly greater than one.

Consider a piecewise linear FHN model with a difference in time scale on the upper and lower branches:

$$g_+(w) = \frac{1-w}{\mu},$$

$$g_-(w) = -w. \tag{19}$$

The values of $h_2, h_3,$ and h_4 parametrized by μ , holding all other parameters fixed, are plotted in Fig. 8 as a solid curve. The curve remains in the stability region for all μ (below the dark gray surface), verified numerically for $\mu \in [1/100, 400]$, but crosses into the predicted unstable region (below the white surface) for $\mu \approx 1.634$. Numerical simulation of this family of FHN systems ($\mu=3,5,7$) with positive ϵ demonstrates that the traveling pulse is stable even for restitution slopes greater than eight (see Fig. 9).

B. “Generalizing” the restitution hypothesis

When trying to understand the dynamics of a complex system, it is often useful to look for simple relationships that describe important features of the system. APD restitution and conduction velocity (CV) restitution are two phenomenological (and experimentally measurable) properties of cardiac tissue that are sometimes used in this way. Conduc-

tion velocity restitution describes the relationship between propagation speed of a front and the preceding diastolic interval in much the same way as APD restitution relates APD to DI. Courtemanche *et al.* parameterize their system using these two properties so that their stability condition is expressed in terms of them. The characteristic equation for their problem is similar to the one derived here. By assuming that the wave back is a phase wave, they essentially assume that APD and DI have zero sensitivity to parameter changes in the wave back. In fact, setting $h_2=h_3=0$ in Eq. (12) we get their characteristic equation,

$$\frac{1-\beta A'}{1+\beta} = \exp\left(\frac{C'}{c_0^2}\beta L\right),$$

where

$$A' = \frac{dAPD}{dDI} = \frac{h_1+h_2}{h_3+h_4} = \frac{h_1}{h_4},$$

$$C' = \frac{dCV}{dDI} = \frac{c_0^2}{h_3+h_4} = \frac{c_0^2}{h_4}, \quad \beta = \alpha h_4$$

(a rescaled eigenvalue).

Notice, as observed by Courtemanche *et al.*, that the image of the left-hand side in the complex β plane is independent of C' , so that the bifurcation curve in the $A'-C'$ parameter space is independent of C' with only the wave numbers of the eigenmodes depend on C' . Recall that this bifurcation is degenerate in the sense that it is always an infinite dimensional Hopf bifurcation.

In reformulating the problem to describe the case of a triggered wave back, we have unfolded the degenerate bifurcation to reveal its generic structure. Using these restitution parameters, the general stability condition becomes

$$A'^2 < 1 + 2 \frac{C'}{c_0^2} (h_2 A' - h_3), \tag{20}$$

$$h_3 A' < h_2. \tag{21}$$

As mentioned, setting $h_2=h_3=0$ gives the restitution condition. Otherwise, the condition is modified by the CV restitution slope. To understand how this modified restitution condition differs from the original restitution condition, we refer to the modified condition in its original form, Eq. (13), and the diagram in Fig. 10.

Suppose we start with a particular FHN system specified by certain parameters which has a traveling pulse solution of unknown stability on the ring. As we change one of the parameters, the pulse changes according to the sensitivities h_i . In Fig. 10, we see an example in which the parameter change shortens the pre-excitation dynamics (h_4) accelerating the arrival of the front at each point on the ring while changes in post-excitation dynamics (h_1) delay the arrival of the front with the net effect being a delay ($h_1 > h_4$). At the back, repolarization is also delayed because $h_3 > h_2$. Referring back to the stability condition, we see that a pulse in this parameter regime is unstable.

Notice that the restitution condition captures this balance of sensitivities at the front but gets it reversed at the back. That is to say that a stabilizing influence at the back (h_2

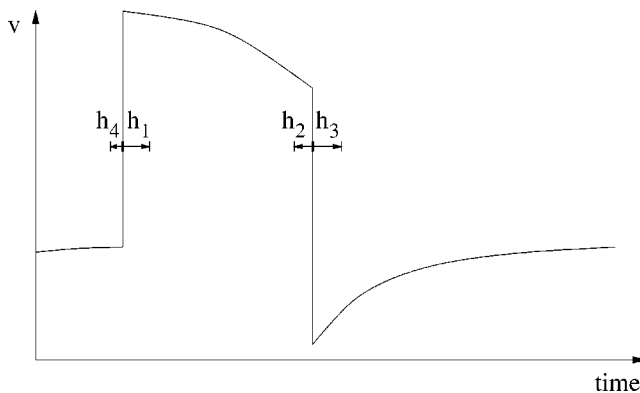


FIG. 10. An action potential at a point on the ring showing the sensitivities (h_i) to parameter changes.

$>h_3$) corresponds to a steepening of the restitution curve. Thus, the restitution condition is only a good approximation to the stability condition when repolarization is insensitive to parameter changes.

The question remains as to whether the restitution condition is a good approximation in actual cardiac tissue. To complement their analytical work which is revisited here, Courtemanche *et al.*²¹ numerically tested the stability of the traveling pulse for the Beeler Reuter model. They found that as ring length is decreased, the length at which stability is lost is well predicted by the restitution condition. We have demonstrated that the restitution condition is an approximation which for some systems might be highly inaccurate. More importantly, by introducing dependence on the CV restitution curve, we provide an analytical description of the source of the deviations from the restitution hypothesis. Thus, even though the restitution condition appears to be accurate for the Beeler Reuter model, a fuller explanation of this accuracy awaits a better understanding of the role of repolarization in stabilizing or destabilizing waves in spatially extended systems.

ACKNOWLEDGMENTS

This research was supported in part by NSF Grant No. DMS-99700876 (J.P.K.) and funding from Fonds pour la Formation de Chercheurs et l'Aide à la Recherche (E.C.). E.C. is grateful to the Sir Isaac Newton Institute for providing office space, resources, and an interactive research environment (including helpful discussions with A. Panfilov).

APPENDIX

1. Phase waves and triggered waves

In this appendix, we focus on some technical calculations which are useful in understanding the difference between a phase wave and a triggered wave. In nontechnical terms, a triggered wave is one in which the spatial coupling of cells plays a role in the wave propagation. A phase wave arises from the coincidental coordination of intrinsic dynamics in neighboring cells. For example, imagine a group of children on a set of swings, all in a line. If each child is pushed in order, after all children have been set in motion, an

apparent wave of bobbing children is seen moving back and forth along the swing-set. This wave is described as a phase wave because the wave motion is not organized by coupling but by the order in which the children are set in motion. Now, if the children all reach out and hold hands, the nature of their motion changes due to the influence each child has on his or her neighbors. This modified wave of motion is a triggered wave. In the latter case, only the first child requires pushing to set the whole group in motion.

In the context of excitable media, a wave front of excitation cannot be a phase wave since the only means by which excitation can occur (without external stimulus) is by cell-cell coupling. On the other hand, a wave back can be a phase wave for the simple reason that deexcitation might occur because of intrinsic dynamics. It might seem like coupling necessarily influences repolarization but in the context of the singular FitzHugh–Nagumo system, this dependence can be relegated to higher order terms when solutions are expressed as power series in ϵ . Thus, we define a phase wave as one in which the *leading order* dynamics of repolarization depend on intrinsic factors only and are not explicitly influenced by coupling. (This classification of waves has been addressed in the context of the Belousov–Zhabotinskii reaction both experimentally²² and theoretically.²³) Physiologically, a phase wave might be defined as one in which the repolarization profile differs from that of an isolated cell by less than some small percentage (of order ϵ). To see how these ideas play out in the singular FitzHugh–Nagumo system, we proceed with a discussion of the inner layer dynamics governed by Eq. (3).

2. The bistable equation

For $0 < W < w_{\max}$, Eq. (3) is a bistable equation meaning it has two spatially uniform stable solutions ($v_+(W)$ and $v_-(W)$). For such a system, the existence and global stability of a traveling wave is well known. This traveling wave has a characteristic speed, c , and shape, $V(z-ct)$ which satisfies $\lim_{z \rightarrow \pm\infty} V(z-ct) = v_{\pm}(W)$ for all t . This convergence result is true for each $0 < W < w_{\max}$ so that we can define the bistable speed function, $c = c(W)$.

This speed function determines the speed of propagation for a jump discontinuity in v located at ϕ with tissue at rest to the left and excited to the right and with $W = w(\phi, 0)$. The speed of a transition layer with reversed orientation (at rest to the right and excited to the left) is given by $-c(W)$. For large values of W (highly refractory tissue), the propagation speed for a transition layer is positive and large, corresponding to propagation that deexcites or repolarizes tissue. Such a wave is referred to as a *wave back*. Similarly, for W small, the speed of propagation is large and negative corresponding to propagation of excitation or depolarization, referred to as a *wave front*.

Notice that a wave back of this type ($0 < W < w_{\max}$) forces cells to repolarize earlier than they would if they were isolated. This is most easily seen in the $v-w$ phase plane. Repolarization of an isolated SFHN cell occurs when the cell reaches the upper end of the excited branch which is at $W = w_{\max}$; a traveling wave of Eq. (3) forces the jump from

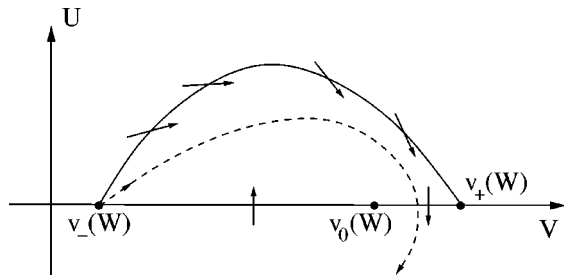


FIG. 11. Phase plane for Eq. (A2) with W and c as described in the text. The solid curve is the traveling wave solution to Eq. (A2) for W which is a heteroclinic trajectory connecting the two saddle points. As the value of c is increased from $c(W)$, the vector field changes from tangential to inward pointing. The V axis is the V nullcline. The vector field along the axis points inward between the lower two critical points and outward between the upper two critical points. The dashed curve is the unstable manifold which always enters the contained region for $c > c(W)$.

excited branch to resting branch to occur at some value of $W < w_{max}$. Thus, a bistable wave back is a triggered wave.

3. The degenerate bistable equation

For $W = w_{max}$, the analysis in the previous section (in particular, the convergence result from Ref. 20) no longer applies. The value $W = w_{max}$ is a bifurcation point for Eq. (3) at which the upper two zeros of $f(v, w)$ collide ($v_0(w_{max}) = v_+(w_{max})$) in a saddle-node bifurcation. We refer to the single degenerate root as $v_+(w_{max})$. Using the existence results from the analysis for the bistable case ($W < w_{max}$), we extend the speed function, $c(W)$, to the degenerate case ($W = w_{max}$).

Changing to traveling coordinates, $\chi = z - ct$, and assuming V is a function of χ only (with V' denoting $dV/d\chi$), Eq. (3) becomes

$$V'' + cV' + f(V, W) = 0. \tag{A1}$$

To facilitate the use of phase plane analysis, we let $U = V'$ which gives the system

$$\begin{aligned} V' &= U, \\ U' &= -cU - f(V, W). \end{aligned} \tag{A2}$$

We look for values of c for which this system has a heteroclinic trajectory connecting $(v_-(w_{max}), 0)$ and $(v_+(w_{max}), 0)$, starting at the former and ending at the latter. The following geometric argument demonstrates the existence of a traveling wave solution for every speed $c > c_{max}$.

Treating W and c as parameters for Eq. (A2), we consider the vector field for any value of W for which $c(W) > 0$ and any $c > c(W)$. Referring to Fig. 13 will be useful in following the construction. For any such pair, we construct a nearly positively invariant region in the phase plane and show that the unstable manifold of the saddle at $(v_-(W), 0)$ enters this region. In order to show the existence of a traveling wave with any speed $c > c_{max}$, we take the limit $W \rightarrow w_{max}$, so that the nearly positively invariant region becomes positively invariant and the unstable manifold of $(v_-(W), 0)$ is squeezed into approaching $(v_+(W), 0)$.

Figure 11 shows the vector field along the boundary of

the proposed nearly positively invariant region for some suitable W and c . The boundary of this region is formed by two curves, the V axis and the traveling wave solution for the chosen value of W . The V axis is actually the V nullcline and between $v_-(W)$ and $v_0(W)$, the vector field points into the positive quadrant. Between $v_0(W)$ and $v_+(W)$, the vector field points in the opposite direction and this interval is the only possible escape from the region under construction. The second curve, which completes the boundary of the nearly invariant region, is the traveling wave (heteroclinic) solution for parameter values W and $c(W)$. Note that this traveling wave is a solution of the system (A2) for $c(W)$ and not for the chosen value of $c > c(W)$. To see the structure of the vector field along the second curve, note that the slope of the vector field is given by

$$\frac{dU}{dV} = -c + \frac{V(V-a)(V-1)}{aU}$$

and is monotone decreasing in c . This guarantees that the vector field, which is tangent to the curve for $c = c(W)$, points inward along the curve for $c > c(W)$. Note that Fig. 11 is the generic phase plane for any value of $W < w_{max}$ for which $c(W) > 0$ and any value of $c > c(W)$.

If the unstable manifold of the saddle at $(v_-(W), 0)$ enters the region, it can only exit along the line segment extending from $(v_0(W), 0)$ to $(v_+(W), 0)$. As $W \rightarrow w_{max}$, this line segment reduces to a point and the unstable manifold necessarily forms a heteroclinic trajectory connecting the saddle at $(v_-(w_{max}), 0)$ and the degenerate saddle-node at $(v_+(w_{max}), 0)$.

As the final step in demonstrating the existence of this infinite family of heteroclinic trajectories, we show that the unstable manifold always enters the nearly invariant region for $c > c(W)$. For $c = c(W)$, the unstable manifold is tangent to the nearly invariant region. As in the case of the vector field, the slope of the unstable manifold as it leaves the point $v_-(W)$ is monotone decreasing in c so that the manifold necessarily enters the nearly invariant region for $c > c(W)$. This is clear by explicit calculation of the eigenvector associated with the unstable manifold:

$$\begin{pmatrix} 2 \\ -c + \sqrt{c^2 + 4} \end{pmatrix}.$$

It is important to note that the traveling wave result for $W = w_{max}$ is different from the traveling wave result for the bistable case ($W < w_{max}$) in that uniqueness is lost. This difference comes from the fact that the traveling wave solution for $W = w_{max}$ is not necessarily a connection between the unstable manifold of one critical point and the stable manifold of the other. Because the heteroclinic trajectory can approach the saddle-node via either the stable manifold (a single trajectory) or the center manifold (a family of trajectories), there is a half ray of traveling waves, one for each $c > c_{max}$, with $c = c_{max}$ corresponding to the stable manifold connection and all others corresponding to center manifold connections (see Fig. 12). This is in contrast with the traveling wave for the bistable case which is a connection between two saddle points in the phase plane.

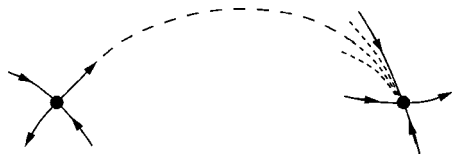


FIG. 12. A schematic representation of the phase plane showing a heteroclinic trajectory connecting the unstable manifold of $(v_-(w_{\max}), 0)$ to the center manifold of $(v_+(w_{\max}), 0)$. The solid curves are stable and unstable manifolds. The dashed curves (short dashes) represent the center manifold of $(v_+(w_{\max}), 0)$ and the dashed curve (long dashes) is the heteroclinic trajectory. The associated traveling wave is a phase wave with $c > c(w_{\max})$ (the connection is via the center manifold).

In addition, it should be emphasized that although the half ray of traveling waves for the degenerate bistable equation is reminiscent of the traveling wave result for the Fisher equation,²⁴ the proof is quite different.

The full relation between W and traveling wave speed is given in two parts as shown in Fig. 13. The first part is the speed function from the bistable equation calculation associated with triggered waves ($0 < W < w_{\max}$) and the second part corresponds to the infinite family of phase waves associated with the degenerate bistable equation ($W = w_{\max}$).

We can now interpret these analytical results in terms of the original discussion of phase waves and triggered waves. As mentioned earlier in this appendix, a phase wave is one in which repolarization is uninfluenced by spatial coupling. In the singular FitzHugh–Nagumo system, this means that repolarization occurs when the recovery variable, w , reaches w_{\max} . In the context of the traveling wave calculations

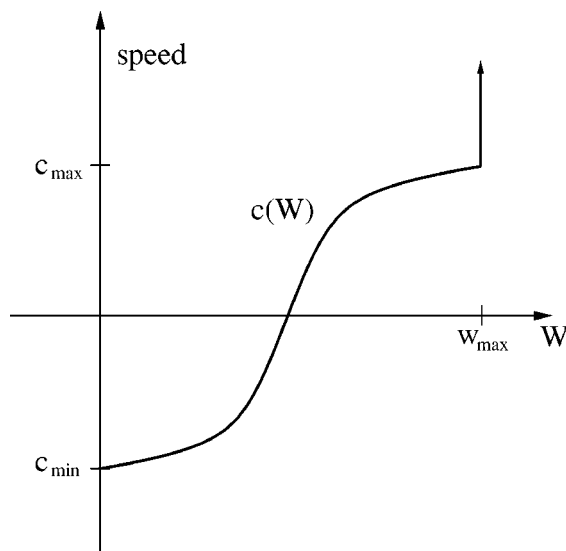


FIG. 13. A schematic representation of the traveling wave speed as a function of W . The speed relationship consists of two parts, the speed function, $c(W)$, associated with triggered waves of the bistable equation ($0 < W < w_{\max}$), and the half ray of speeds ($c > c_{\max}$) associated with phase waves of the degenerate bistable equation ($W = w_{\max}$).

above, we see that traveling wave solutions to the bistable equation fall under the category of triggered waves while solutions to the degenerate bistable equation are phase waves.

- ¹F. Fenton, S. Evans, and H. Hastings, “Memory in an excitable medium: A mechanism for spiral wave breakup in the low-excitability limit,” *Phys. Rev. Lett.* **83**, 3964–3967 (1999).
- ²F. Fenton and A. Karma, “Vortex dynamics in three-dimensional continuous myocardium with fiber rotation: Filament instability and fibrillation,” *Chaos* **8**, 20–47 (1998).
- ³A. V. Panfilov and J. P. Keener, “Re-entry in three-dimensional myocardium with rotational anisotropy,” *Physica D* **84**, 545–552 (1995).
- ⁴A. V. Panfilov and P. Hogeweg, “Spiral breakup in a modified FitzHugh–Nagumo model,” *Phys. Lett. A* **176**, 295–299 (1993).
- ⁵A. Panfilov and A. Pertsov, “Ventricular fibrillation: Evolution of the multiple-wavelet hypothesis,” *Philos. Trans. R. Soc. London* **359**, 1315–1325 (2001).
- ⁶A. Garfinkel, Y. H. Kim, O. Voroshilovsky, Z. Qu, J. R. Kil, M. H. Lee, H. S. Karagueuzian, J. N. Weiss, and P. S. Chen, “Preventing ventricular fibrillation by flattening cardiac restitution,” *Proc. Natl. Acad. Sci. USA* **97**, 6061–6066 (2000).
- ⁷M. Riccio, M. Koller, and R. Gilmour, Jr., “Electrical restitution and spatiotemporal organization during ventricular fibrillation,” *Circ. Res.* **84**, 955–963 (1999).
- ⁸M. Koller, M. Riccio, and R. Gilmour, Jr., “Dynamic restitution of action potential duration during electrical alternans and ventricular fibrillation,” *Am. J. Physiol.* **275**, H1635–H1642 (1998).
- ⁹A. Karma, “Spiral breakup in model equations of action potential propagation in cardiac tissue,” *Phys. Rev. Lett.* **71**, 1103–1106 (1993).
- ¹⁰Z. Qu, J. Weiss, and A. Garfinkel, “Cardiac electrical restitution properties and stability of reentrant spiral waves: A simulation study,” *Am. J. Physiol.* **276**, H269–H283 (1999).
- ¹¹M. Courtemanche, J. P. Keener, and L. Glass, “A delay equation representation of pulse circulation on a ring in excitable media,” *SIAM (Soc. Ind. Appl. Math.) J. Appl. Math.* **56**, 119–142 (1996).
- ¹²A. Karma, H. Levine, and X. Zou, “Theory of pulse instabilities in electrophysiological models of excitable tissues,” *Physica D* **73**, 113–127 (1994).
- ¹³A. Karma, “New paradigm for drug therapies of cardiac fibrillation,” *Proc. Natl. Acad. Sci. USA* **97**, 5687–5689 (2000).
- ¹⁴J. B. Nolasco and R. W. Dahlen, “A graphic method for the study of alternation in cardiac action potentials,” *J. Appl. Physiol.* **25**, 191–196 (1968).
- ¹⁵M. R. Guevara, G. Ward, A. Shrier, and L. Glass, “Electrical alternans and period-doubling bifurcations,” in *Computers in Cardiology* (IEEE, New York, 1984).
- ¹⁶A. R. Yehia, D. Jeandupeux, F. Alonso, and M. R. Guevara, “Hysteresis and bistability in the direct transition from 1:1 to 2:1 rhythm in periodically driven single ventricular cells,” *Chaos* **9**, 916–931 (1999).
- ¹⁷G. R. Mines, “On circulating excitations in heart muscles and their possible relation to tachycardia and fibrillation,” *Trans. R. Soc. Can.* **4**, 43–53 (1914).
- ¹⁸A. Karma, “Electrical alternans and spiral wave breakup in cardiac tissue,” *Chaos* **4**, 461–472 (1994).
- ¹⁹A. Vinet, “Quasiperiodic circus movement in a loop model of cardiac tissue: Multistability and low dimensional equivalence,” *Ann. Biomed. Eng.* **28**, 704–720 (2000).
- ²⁰P. C. Fife and J. B. McLeod, “The approach of solutions of nonlinear diffusion equations to traveling front solutions,” *Arch. Ration. Mech. Anal.* **65**, 335–361 (1977).
- ²¹M. Courtemanche, J. P. Keener, and L. Glass, “Instabilities of a propagating pulse in a ring of excitable media,” *Phys. Rev. Lett.* **70**, 2182–2185 (1993).
- ²²A. T. Winfree, “Two kinds of waves in an oscillating chemical solution,” *Faraday Symp. Chem. Soc.* **9**, 38–46 (1974).
- ²³J. J. Tyson and P. C. Fife, “Target patterns in a realistic model of the Belousov–Zhabotinskii reaction,” *J. Chem. Phys.* **73**, 2224–2237 (1980).
- ²⁴R. A. Fisher, “The wave of advance of advantageous genes,” *Ann. Eugenics* **7**, 353–369 (1937).